CHEMISTRY & CHEMICAL TECHNOLOGY

Chem. Chem. Technol., 2025,
Vol. 19, No. 4, pp. 735–750

Chemical Technology

STUDY OF THE INFLUENCE OF POLYAMIDE FILLER ON THE PHYSICAL AND MECHANICAL PROPERTIES OF HIGH-STRENGTH CONCRETE

Orest Vakhula[1,✉], Volodymyr Moravskyi[1], Oleksandr Grytsenko[1], Diana Kindzera[1]

[1] Lviv Polytechnic National University, 12, S. Bandery str., Lviv, 79013, Ukraine
✉ *orest.m.vakhula@lpnu.ua*

https://doi.org/10.23939/chcht19.04.735

Abstract. The article investigates the influence of various polyamide fillers (granulated polyamide PA-6, polyamide fibers, and polyamide waste) on the physico-mechanical properties of high-strength concrete. It has been established that surface modification of the fillers using inorganic salt solutions ($CaCl_2$, $Al_2(SO_4)_3$, and $Ca(NO_3)_2$) can affect the hydration processes of the cement matrix and enhance interfacial interactions, which in turn improve the strength and durability of the concrete. The highest compressive strength ($f_{cs}2$= 72.8 MPa; $f_{cs}28$ = 106.4 MPa) was achieved using 10 wt. % of PA-6 granules and 1.0 wt. % of fibers modified in a 30 % $CaCl_2$ solution. This combination provides effective reinforcement of the concrete structure, reduces the likelihood of crack formation, and contributes to improved performance characteristics. Additionally, the use of polyamide waste as a filler represents a promising approach to polymer material recycling with a positive environmental impact.

Keywords: cement system, high-strength concrete, polyamide, polyamide fiber, polyamide waste, strength.

1. Introduction

High-strength concrete (HSC) is a specialized type of concrete known for its superior mechanical properties, making it ideal for constructing demanding structures such as bridges, skyscrapers, large-scale buildings, and components exposed to aggressive environments.[1] HSC is characterized by a higher strength-to-weight ratio, lower permeability, and reduced creep and shrinkage compared to normal-strength concrete (NSC).[2] One key distinction between HSC and NSC is HSC's lower water-to-binder ratio, which enhances its strength and durability.[3] Concrete is typically classified as HSC when its compressive strength reaches or exceeds 60 MPa.[4] The growing interest in HSC is driven by its exceptional compressive strength, unique microstructure, reduced porosity, and enhanced durability.[5] High-strength building materials, including HSC and high-strength steel (with a yield strength of at least 460 N/mm²), are widely used in construction engineering to meet the demands of modern infrastructure.[6]

Improvements in the operational properties of concrete are achieved through its modification with various additives, among which polymer materials are widely used.[7] Depending on their nature, these additives improve the plasticity, strength, and heat resistance of the cement composite. Currently, the most commonly used synthetic polymers for enhancing the physical and mechanical properties of cement composites are polyethylene, polypropylene, and polyvinyl alcohol.[8]

Due to their unique properties, polyamides are considered promising fillers for concrete. The presence of polar amide groups in their macromolecules leads to strong intermolecular interactions through hydrogen bonding, giving polyamides a combination of characteristics such as wettability, chemical resistance, elasticity, and high mechanical strength.[9, 10] These features make them suitable for creating composite materials with enhanced operational characteristics.[11–13]

The inclusion of polyamide fillers in concrete composites is expected to improve the material's heat resistance, strength, and crack resistance. To enhance the strengthening effect, this study proposes modifying the surface of the polyamide fillers with inorganic salts of various types.

At the same time, the disposal of polyamide-based polymer waste has become a pressing environmental issue. Polyamide waste (*e. g.*, nylon) poses significant environmental challenges due to its durability, low biodegradability, and the complexity of its recycling.[14] Major concerns include the slow decomposition of such waste and its accumulation in ecosystems. Used polyamide products – such as textile fibers, fishing nets, and packaging – often end up in water bodies, harming marine ecosystems. Another serious issue is that the degradation of polyamide materials leads to the formation of micro- and nanoplastic particles, which enter water, soil, and the food chain. Therefore, finding effective solutions for the disposal of polyamide waste is an essential, one of which could be incorporating such waste into concrete mixtures.[15, 16]

The aim of this study is to investigate the effects of various types of polyamide fillers (granules, fibers, and waste particles), particularly those that have been modified, on the physical and mechanical properties of cement composites, and to create modified high-strength concrete with improved construction and technical characteristics on this basis.

2. Experimental

2.1. Materials

Portland cement (PC) PC I-500R-N, manufactured by PrJSC "Ivano-Frankivskcement", was used to prepare the concrete mixture based on Portland cement clinker with a standardized mineralogical composition and fine sand from the Mykolaiv deposit (Lviv region, ρ_{bulk} = 1370 kg/m^3). The mixture was modified with the superplasticizer MasterSure HES 1515, based on polycarboxylate esters and produced by Master Builders Solutions (Poland, $\rho = 1.09 \pm 0.02$ g/cm^3, pH = 9.0 ± 1.0), to enhance the strength of the cementing system due to its significant water-reducing effect.

The composition of the concrete mixture is characterized by the following quantitative content of components, calculated per 1 m^3: PC = 800 kg, sand = 1400 kg, MasterSure HES 1515 = 12 kg (1.5 % by mass of cement), water = 200 kg, *W/C* = 0.25 (control composition). The mixture was compacted in molds under constant vibration parameters without additional loading, using a standard vibrating table operating at 3000 oscillations per minute. The workability of the concrete mixture in its basic composition was characterized by a cone slump of 165.0 mm.

For the research, granulated polyamide PA-6 (Fig. 1, *a*) of the TECHNYL C 216 V30 NC grade, produced by DOMO Chemicals (Germany), was used. This material contains 30 % fiberglass, has a density of 1.36 g/cm^3, and a flexural strength of 250 MPa. The maximum initial moisture content of the granules did not exceed 0.2 %.

Polyamide microfibers "Virtuoz AV-1" (produced by "Virtuoz", Ukraine), used in the study, were 4 mm in length (Fig. 1, *b*).

The waste material used in the study consisted of shredded technological waste (defective products) from the manufacturing of household electrical appliance components, provided by LLC "Electronpobutprylad Plant" (Lviv, Ukraine) and made of glass-filled polyamide PA-6, TECHNYL C 216 V30 NC grade (DOMO Chemicals, Germany). The waste (Fig. 1c) appeared as irregularly shaped, plate-like fragments with overall dimensions of width × length = 3–10 × 4–15 mm and a thickness of 0.3–0.8 mm.

a b c

Fig. 1. Polyamide filler: a – granules; b – fiber; c – polyamide waste

The following chemical compounds were used as salts for the preparation of modifying solutions:

– reagent grade aluminum sulfate ($Al_2(SO_4)_3 \cdot 18\,H_2O$, AS) CAS Nr: 7784-31-8 manufactured by Sigma-Aldrich (USA);

– Calcium chloride ($CaCl_2$) CAS Nr: 10043-52-4 manufactured by Kuhlmann Europe (Belgium).

– Calcium nitrate ($Ca(NO_3)_2 \cdot 4H_2O$) CAS Nr: 13477-134-4 manufactured by WEGO Chemical Group (USA).

2.2. Methods

The modification of the surfaces of polyamide fillers (PA-6 granules and polyamide fibers) involved hydrating the hydrogen bonds between macromolecules. This was achieved by immersing the PA-6 granules and fibers in modifying solutions for 120 hours. The granules were treated with distilled water and 30 % aqueous solutions of calcium chloride ($CaCl_2$), aluminum sulfate ($Al_2(SO_4)_3$), and calcium nitrate ($Ca(NO_3)_2$). The fibers were modified using 30 % solutions of $CaCl_2$ and $Al_2(SO_4)_3$. The modification process included the following stages (Fig. 2): immersion of the fillers (PA-6 granules or fibers) in the modifying solution for 120 hours; removal of excess moisture from the surfaces of the fillers; preparation of the concrete mixture with the modified fillers; pouring the concrete mixture into molds for further curing and testing.

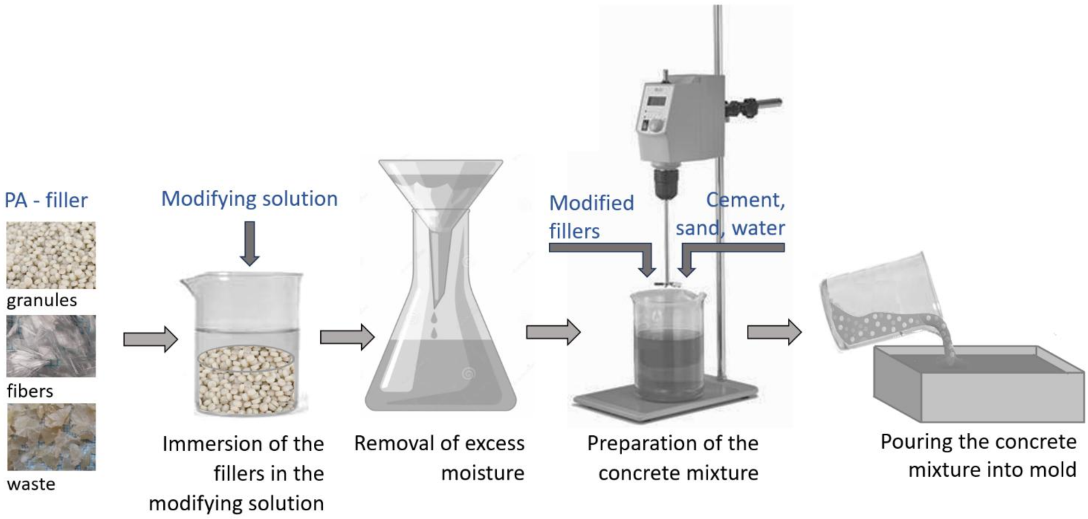

Fig. 2. Schematic diagram of the modification process for polyamide fillers and the preparation of the concrete mixture

To characterize changes in the chemical structure and conformation of polyamide macromolecules, IR spectroscopic analysis was performed using a Spectrum Two spectrophotometer (PerkinElmer, UK) equipped with a diamond attenuated total reflection (UATR) accessory. The spectral resolution was 0.4 cm^{-1}, the scanning range extended from 4000 cm^{-1} to 400 cm^{-1}, and 32 scans were recorded. The obtained spectra were interpreted using Fourier transform analysis.

Scanning electron microscopy (SEM) was conducted using the raster microscope of the REMMA-102-02 electron microanalyzer (SELMI, Ukraine) to examine the shape of the crystals formed in the cement matrix and to study the microstructure of concrete samples after 7 days of curing.

The compressive strength class of the concrete was determined in accordance with DSTU B V.2.7-239:2010 (EN 1015-11:1999, NEQ “Methods of test for mortar for masonry – Part 11: Determination of flexural and compressive strength of hardened mortar”), using prism samples with a square cross-section of 40×40×160 mm. These samples were tested after bending, as per DSTU B V.2.7-187 (ISO 1920-4:2020 “Testing of concrete Part 4: Strength of hardened concrete”), and were prepared and aged under standard conditions according to DSTU B V.2.7-224 (EN 12390-2:2019 “Testing hardened concrete – Part 2: Making and curing specimens for strength tests”).

3. Results and Discussion

Polymer concretes are produced by partially replacing coarse or fine aggregates with polymers (or polymer particles) of various types.[17] However, the incorporation of polymer fillers often results in reduced mechanical properties of concrete due to the incompatibility between the filler and the cement matrix. This issue stems from the hydrophobic nature and smooth surfaces of polymer particles, which hinder effective bonding with the matrix.[18]

To modify the structure of concrete, granulated polyamide PA6 was added to the basic composition in an amount of 10 wt. % relative to the mass of cement. An SEM image of a PA-6 granule embedded in the concrete matrix is shown in Fig. 3.

For concrete samples with the researched composition, compressive strength is $f_{cs}2$ = 61.2 MPa at an early age (2 days), increasing to $f_{cs}28$ = 92.8 MPa after 28 days of curing (Fig. 4). The flexural tensile strength was $f_{fs}2$ = 9.41 MPa at 2 days and rose to $f_{fs}28$ = 11.6 MPa at 28 days (Fig. 5).

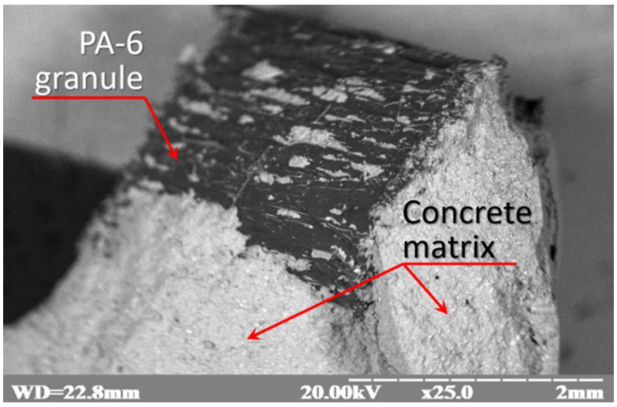

Fig. 3. SEM image of a PA-6 granule embedded in the concrete matrix

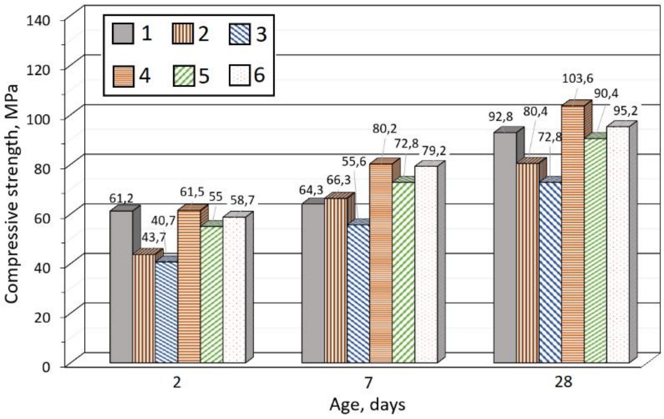

Fig. 4. Compressive strength of concrete samples: 1 – without polyamide granules; 2 – with the addition of unmodified PA-6 polyamide granules; 3 – with the addition of PA-6 polyamide granules modified in distilled water; 4 – with the addition of PA-6 polyamide granules modified in $CaCl_2$ solution; 5 – with the addition of PA-6 polyamide granules modified in Ca $(NO_3)_2$ solution; 6 – with the addition PA-6 polyamide granules modified in $Al_2(SO_4)_3$ solution

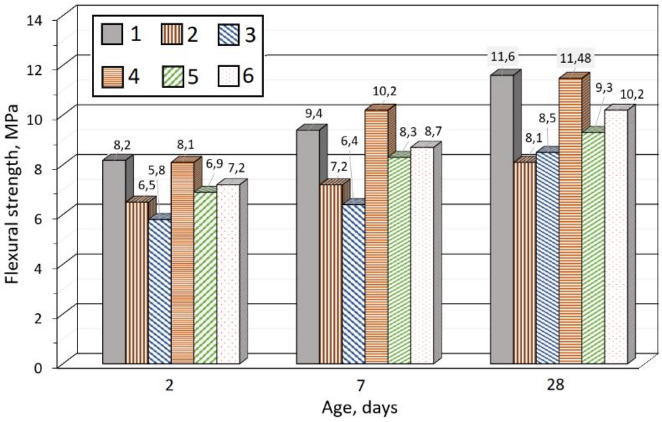

Fig. 5. Flexural tensile strength of concrete samples: 1 – without polyamide granules; 2 – with the addition of unmodified PA-6 granules; 3 – with the addition of PA-6 granules modified in distilled water; 4 – with the addition of PA-6 granules modified in $CaCl_2$ solution; 5 – with the addition of PA-6 granules modified in Ca $(NO_3)_2$ solution; 6 – with the addition PA-6 granules modified in $Al_2(SO_4)_3$ solution

Polyamide (PA) is a linear polymer characterized by repeating amide bonds (–CO–NH–) along its molecular chain. PA is widely known for its outstanding properties, including high tensile strength, electrical insulation, heat resistance, and biocompatibility.[19] It exhibits excellent mechanical characteristics such as a high modulus of elasticity, notable hardness, and strong abrasion resistance, along with relatively high viscosity.[20] Additionally, PA-6 is a thermoplastic, partially crystalline material produced via the polycondensation of ε-aminocaprolactam. A key benefit of PA-6 is its suitability for thermal processing and its utility as a base material for polymer composites.[21] PA-6 is a well-known semi-crystalline polymer with two primary crystalline forms: α and γ phases.[22] Its crystalline structure contributes to its excellent mechanical, barrier, and thermal properties. Under dry conditions, polar groups in the polymer chains form hydrogen bonds via intra- and intermolecular interactions, significantly enhancing the material's strength. However, hydration disrupts some of these hydrogen bonds between polymer chains and forms new bonds with water molecules.[23, 24]

For the concrete containing unmodified PA-6 granules, the compressive strength at the age of 2 days was $f_{cs}2$ = 43.7 MPa, increasing to $f_{cs}28$ = 80.4 MPa after 28 days of curing (Fig. 4). The flexural tensile strength was $f_{fs}2$ = 6.5 MPa at 2 days, reaching $f_{fs}28$ = 8.1 MPa after 28 days (Fig. 5).

The properties of polyamide fillers can be significantly enhanced by surface modification. PA-6 granules were pretreated in distilled water and 30 % aqueous solutions of salts, including calcium chloride ($CaCl_2$), aluminum sulfate ($Al_2(SO_4)_3$), and calcium nitrate ($Ca(NO_3)_2$), and then incorporated into the concrete mixture at a dosage of 10 % by cement mass.

Following immersion in these solutions, the granules were analyzed via FTIR spectroscopy to characterize their structural changes (Fig. 6). This analysis revealed spectroscopic differences between the original and salt-treated granules, providing insights into vibrational characteristics of specific functional groups. These findings are crucial for interpreting possible molecular interactions within the modified composite material.

PA-6 is a semi-crystalline polymer capable of crystallizing into stable α and γ forms, as well as an unstable β form. Its molecular structure comprises pentamethylene segments ($–(CH_2)_5–$) separated by secondary amide groups (–NH–CO–). The presence of amide bonds allows for hydrogen bonding between macromolecular chains, contributing to the formation of planar surfaces.

In the α-crystalline form, hydrogen bonds are established between antiparallel macromolecular chains, whereas in the γ-crystalline phase, they form between parallel chains. The primary difference between these two crystalline structures lies in the distance between repeating segments – 1.724 nm for the α form and 1.688 nm for the γ form – arising from their distinct conformations: planar in α and helical in γ. The β-crystalline form is characterized by a disordered conformation with a repeating segment distance of approximately 1.67 nm.[25] The spectral bands associated with amide groups are primarily influenced by the arrangement of hydrogen bonds, while the vibrational modes of methylene groups are indicative of the overall chain conformation.[25]

The spectrum of the original PA-6 granules, shown in Fig. 6, *a*, contains absorption bands at 834, 929, 960, and 1200 cm^{-1}, clearly indicating the presence of the α-crystalline form. Additionally, the absence of bands at 976 and 1436 cm^{-1} – typically associated with the γ-crystalline form – further confirms the predominance of the α-phase.[25]

As a semi-hydrophobic polymer, polyamide is capable of adsorbing various ions from aqueous solutions,[26] a phenomenon that should be reflected in the spectra of modified samples. Metal ions exhibit a strong tendency to coordinate with amide groups, enabling interaction with polyamide macromolecules. These ions may also directly coordinate with the carbonyl oxygen atoms in the amide groups.[27]

Spectral analysis comparing the original granules with those modified in aqueous salt solutions reveals broadening and increased absorption in the bands associated with amide A and amide B vibrations (Fig. 6, *b*) in the treated samples. Notably, the positions of the amide A and B bands remain unchanged. The amide A band is linked to N–H stretching vibrations and reflects the overall hydrogen bonding involving N–H groups. Its broadening and increased intensity in the modified samples indicate an enhancement in hydrogen bonding. Additionally, an increase in the intensity of the amide I and amide II bands is observed (Fig. 6, *c*). The amide I band primarily arises from the C=O stretching vibration in the polyamide backbone, while the amide II band corresponds to in-plane N–H bending vibrations. The amide I band is highly sensitive to slight changes in molecular geometry, whereas the amide II band is influenced by chain conformation and intermolecular hydrogen bonding, offering insight into the distribution and strength of hydrogen bonds. The enhanced intensity of both amide I and amide II bands suggests the formation of coordination bonds between polyamide macromolecules and metal ions. These bonds penetrate the polyamide structure due to the partial release of C=O and N-H groups from hydrogen bonds initially formed between parallel polyamide macromolecules. Metal ions likely create additional vibrational states, which, in turn, enhance the intensity of the two amide peaks. The increase in the intensity of the amide I and amide II bands suggests that coordination between polyamide and metal ions occurs through CO-NH groups.

For concrete samples containing modified polyamide granules in an $Al_2(SO_4)_3$ solution, the compressive strength on the second day of hardening is $f_{cs}2 = 58.7$ MPa, and after 28 of concrete in bending, in this case days of hardening, it reaches $f_{cs}28 = 95.2$ MPa (Fig. 4). The tensile strength, is $f_{fs}2=7.2$ MPa on the second day and $f_{fs}28 = 10.2$ MPa after 28 days (Fig. 5). For concrete samples containing modified polyamide granules in a $Ca(NO_3)_2$ solution, the compressive strength on the second day of hardening is $f_{cs}2 = 55.0$ MPa, and after 28 days, it is $f_{cs}28 = 90.4$ MPa (Fig. 4). The tensile strength in bending for this composition is $f_{fs}2 = 6.9$ MPa on the second day and $f_{fs}28 = 9.3$ MPa after 28 days (Fig. 5).

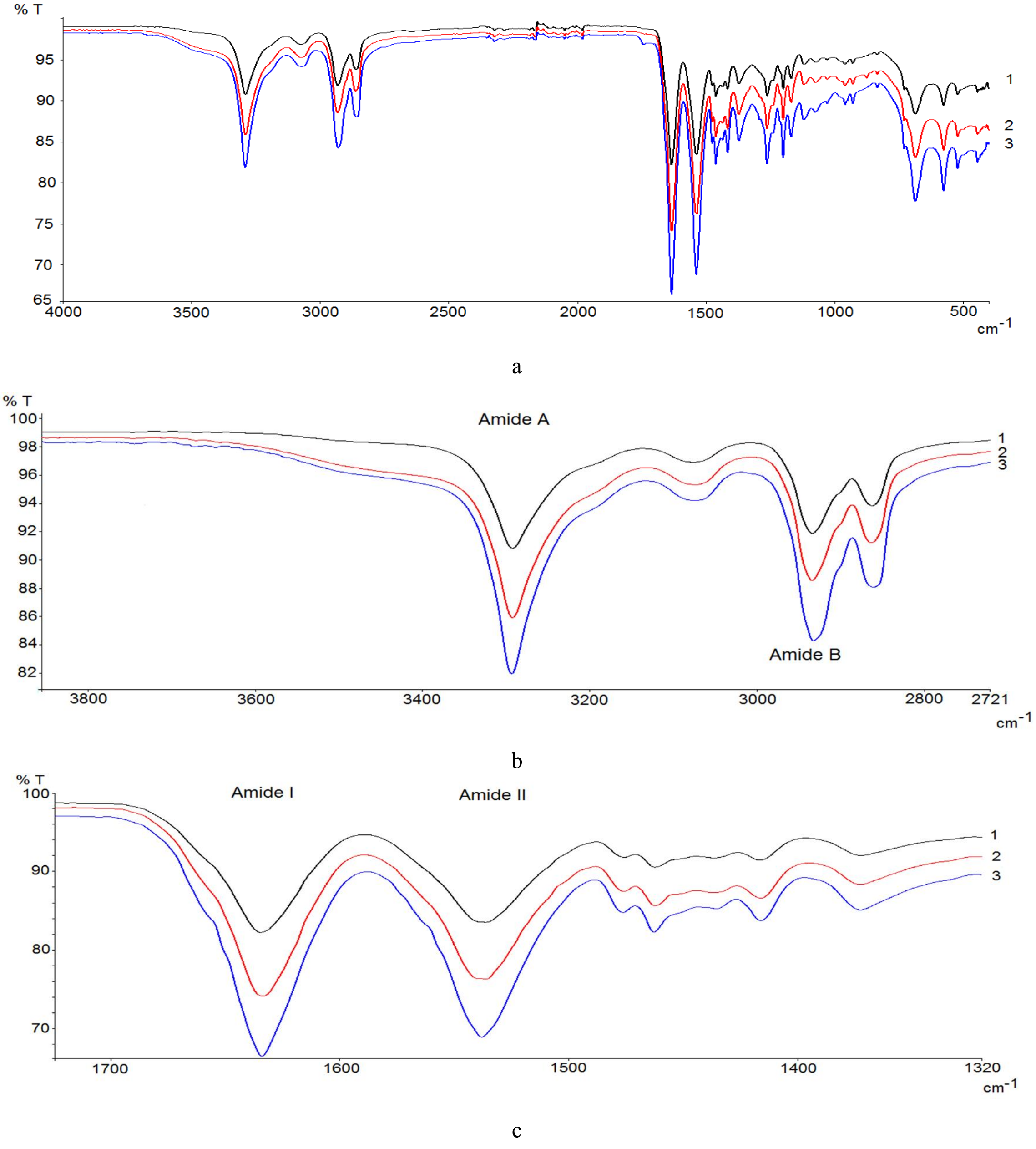

Fig. 6. FTIR spectras of granules of the original polyamide (1), granules modified in the $CaCl_2$ solution (2), granules modified in the $Al_2(SO_4)_3$ solution (3) in the ranges: a – 400–4000 cm^{-1}; b – 2721–3855 cm^{-1}; c – 1320–1724 cm^{-1}

As shown in Fig. 4, the highest compressive strength of the concrete samples is achieved on the second day of hardening, reaching $f_{cs}2$ = 61.5 MPa**.** After 28 days of hardening, the compressive strength further increases to $f_{cs}28$ = 103.6 MPa**.** These strength values correspond to concrete containing 10 % by mass of PA-6 polyamide granules modified in a $CaCl_2$ solution. The flexural tensile strength of this concrete was $f_{fs}2$ = 8.1 MPa at 2 days and increased to $f_{fs}28$ = 11.4 MPa after 28 days (Fig. 5). In contrast, the lowest compressive strength is observed in concrete samples containing PA-6 polyamide granules modified in distilled water. At an early age, the compressive strength for these samples is $f_{cs}2$ = 40.7 MPa, and after 28 days of hardening, it reaches $f_{cs}28$ = 72.8 MPa (Fig. 4). The flexural tensile strength of this concrete was $f_{fs}2$ = 5.8 MPa at 2 days and increased to $f_{fs}28$ = 8.5 MPa after 28 days (Fig. 5). These findings demonstrate that modifying polyamide granules with calcium chloride significantly enhances the mechanical properties of concrete, while modification with distilled water yields the least improvement.

The mechanical properties of concrete, as a composite material, are significantly influenced by the compatibility and bond strength between the fillers and the cement matrix. Consequently, failure in composite materials most commonly occurs at the polyamide (PA) / concrete phase interface, specifically within the Interfacial Transition Zone (ITZ) of the concrete (Fig. 7).

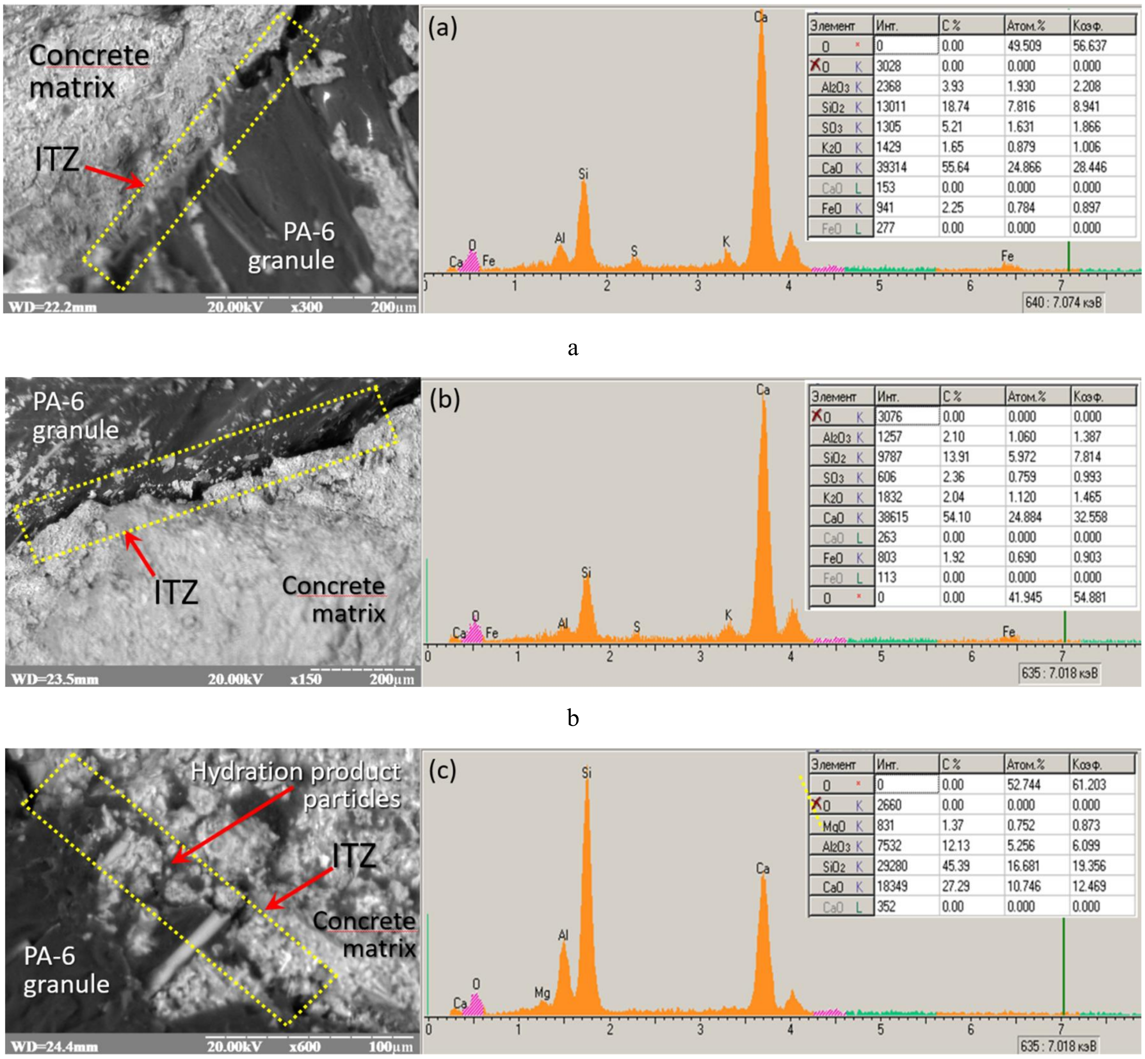

Элемент	Инт.	C %	Атом.%	Коэф.
O	0	0.00	49.509	56.637
O K	3028	0.00	0.000	0.000
Al_2O_3 K	2368	3.93	1.930	2.208
SiO_2 K	13011	18.74	7.816	8.941
SO_3 K	1305	5.21	1.631	1.866
K_2O K	1429	1.65	0.879	1.006
CaO K	39314	55.64	24.866	28.446
CaO L	153	0.00	0.000	0.000
FeO K	941	2.25	0.784	0.897
FeO L	277	0.00	0.000	0.000

a

Элемент	Инт.	C %	Атом.%	Коэф.
O K	3076	0.00	0.000	0.000
Al_2O_3 K	1257	2.10	1.060	1.387
SiO_2 K	9787	13.91	5.972	7.814
SO_3 K	606	2.36	0.759	0.993
K_2O K	1832	2.04	1.120	1.465
CaO K	38615	54.10	24.884	32.558
CaO L	263	0.00	0.000	0.000
FeO K	803	1.92	0.690	0.903
FeO L	113	0.00	0.000	0.000
O	0	0.00	41.945	54.881

b

Элемент	Инт.	C %	Атом.%	Коэф.
O	0	0.00	52.744	61.203
O K	2660	0.00	0.000	0.000
MgO K	831	1.37	0.752	0.873
Al_2O_3 K	7532	12.13	5.256	6.099
SiO_2 K	29280	45.39	16.681	19.356
CaO K	18349	27.29	10.746	12.469
CaO L	352	0.00	0.000	0.000

c

Fig. 7. SEM images of the contact zone between the concrete matrix and PA-6 granule:
a – unmodified PA-6 granule; b – PA-6 granule modified in distilled water;
c – PA-6 granule modified in $Ca(NO_3)_2$ solution

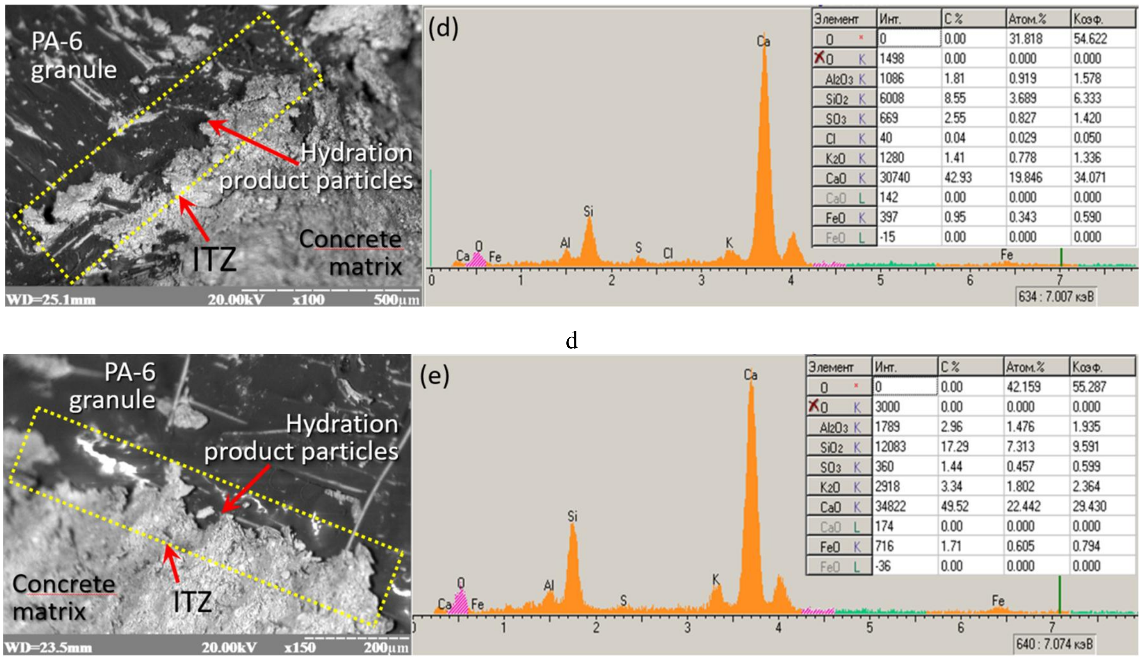

Элемент	Инт.	C %	Атом.%	Коэф.
O ×	0	0.00	31.818	54.622
✗O K	1498	0.00	0.000	0.000
Al_2O_3 K	1086	1.81	0.919	1.578
SiO_2 K	6008	8.55	3.689	6.333
SO_3 K	669	2.55	0.827	1.420
Cl K	40	0.04	0.029	0.050
K_2O K	1280	1.41	0.778	1.336
CaO K	30740	42.93	19.846	34.071
CaO L	142	0.00	0.000	0.000
FeO K	397	0.95	0.343	0.590
FeO L	-15	0.00	0.000	0.000

d

Элемент	Инт.	C %	Атом.%	Коэф.
O ×	0	0.00	42.159	55.287
✗O K	3000	0.00	0.000	0.000
Al_2O_3 K	1789	2.96	1.476	1.935
SiO_2 K	12083	17.29	7.313	9.591
SO_3 K	360	1.44	0.457	0.599
K_2O K	2918	3.34	1.802	2.364
CaO K	34822	49.52	22.442	29.430
CaO L	174	0.00	0.000	0.000
FeO K	716	1.71	0.605	0.794
FeO L	-36	0.00	0.000	0.000

e

Fig. 7. (*Continuation*) SEM images of the contact zone between the concrete matrix and PA-6 granule: d – PA-6 granule modified in $CaCl_2$ solution; e – PA-6 granule modified in $Al_2(SO_4)_3$ solution; and a–e – EDX spectras of the surfaces

Unlike conventional concrete fillers such as sand, crushed stone, or gravel, polymer fillers typically possess hydrophobic properties and smooth surfaces. These characteristics lead to the development of a weaker ITZ with the cement matrix.[28] Fig. 7, *a–e* presents the energy-dispersive X-ray spectroscopy (EDX) analysis of PA-6 granules, along with line scans across the interfacial transition zone (ITZ) between the polyamide granule and the concrete matrix. The EDX maps show the distribution of specific elements: calcium (Ca), silicon (Si), oxygen (O), and carbon (C). The scan line passes through the ITZs, covering the cement layers. Within the ITZ layers, in addition to Ca derived from cement hydration, a noticeable increase in Si concentration is observed.

The absence of a contact zone between the polyamide granule modified in distilled water and the concrete matrix (Fig. 7, *b*) can be attributed to the polyamide's water absorption, which negatively affects the polymer's properties. Ksouri and de Almeida reported[29] that water molecules penetrating between the amine and carbonyl groups of the polyamide weaken or break the secondary bonds between these polar groups. As a result, hydrogen-bonded polymers such as polyamide become highly sensitive to moisture. The degradation in tensile strength and tensile modulus of PA-6 due to moisture can reach approximately 90 %.[30] As previously noted, the polar groups in polyamide can form hydrogen bonds both with other polymer molecules and with components of the concrete mixture. This phenomenon highlights the critical importance of proper surface modification to enhance the performance of polyamide fillers in composite materials.

In this study, water and aqueous salt solutions were used to modify the surface of the polyamide granules. When water was used, surface modification occurred due to the disruption of intermolecular hydrogen bonds on the polymer surface and the formation of new bonds with water molecules (Fig. 8).

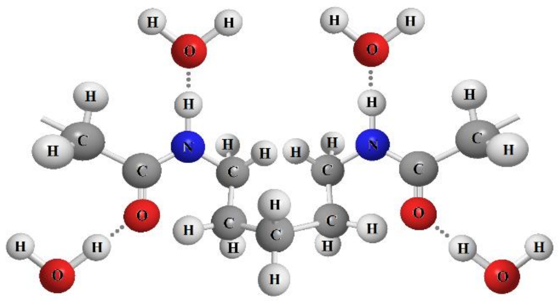

Fig. 8. Schematic formation of intermolecular hydrogen bonds with water molecules on the polyamide surface

This restructuring of the polyamide surface resulted in a lower density, making it more capable of adsorbing dissolved salt ions from aqueous solutions (Fig. 9).

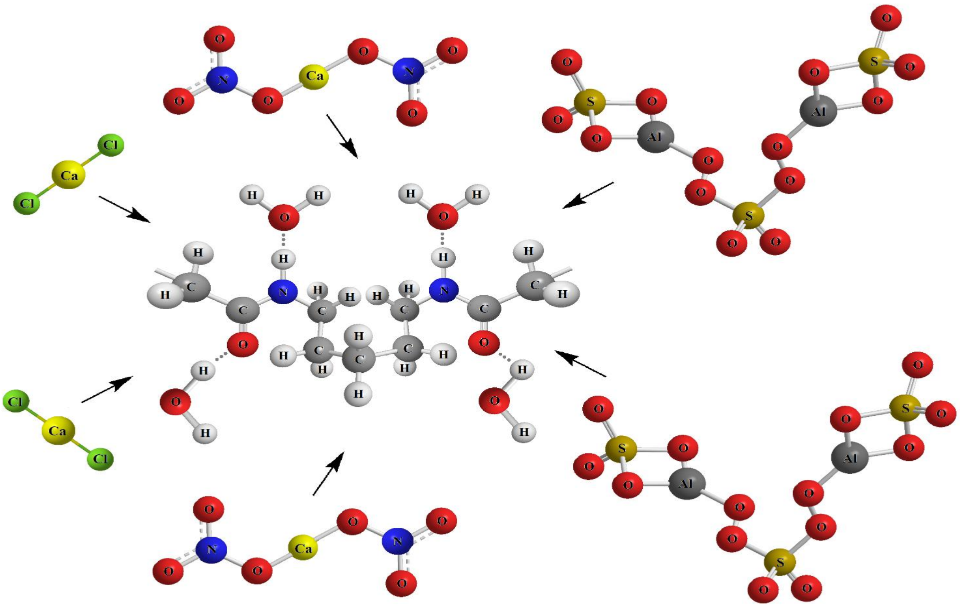

Fig. 9. Scheme of sorption interaction of dissolved salt ions with polyamide

The presence of salt ions in the surface layers of polyamide, which significantly influence hydration processes and structure formation, is expected to affect the properties of cement systems. Specifically, in the case of polyamide granules saturated with salt solutions, the impact of these ions is likely to manifest at the "polymer surface – cement system distribution boundary".

The lowest compressive strength was observed in concrete samples containing 10 % by weight of PA-6 granules modified in distilled water. In contrast, slightly higher compressive strength was recorded in concrete incorporating PA-6 granules modified in a 30 % calcium nitrate ($Ca(NO_3)_2$) solution. The highest compressive strength was achieved in concrete samples containing PA-6 granules modified in 30 % solutions of calcium chloride ($CaCl_2$) and aluminum sulfate ($Al_2(SO_4)_3$).

Due to the hygroscopic nature of PA-6, the moisture diffusion can alter the properties of the polymer. The transport of water has a significant effect on the structure, morphology, and physical characteristics of polymers.[31] When PA-6 is immersed in water, it becomes saturated, and the water content can increase to approximately 9 % by weight.[32]

PA-6 is capable to adsorb salt ions $Ca^{2+}Cl^{2-}$, $Ca^{2+}(NO_3)^{2-}$ and $Al^{3+}{}_2(SO_4)^{2-}{}_3$ from aqueous modifying solutions such as calcium chloride ($CaCl_2$), aluminum sulfate ($Al_2(SO_4)_3$), and calcium nitrate ($Ca(NO_3)_2$) onto its active surface (Fig. 9). Under the influence of cement hydration – a process accompanied by exothermic heat release – polyamide granules modified with 30 % aqueous solutions of these salts are capable of desorbing the adsorbed ions $Ca^{2+}Cl^{2-}$, $Ca^{2+}(NO_3)^{2-}$ and $Al^{3+}{}_2(SO_4)^{2-}{}_3$ from their surface layers into the cement matrix, thereby ensuring the formation of localized zones where hydration processes are accelerated at the interface between the polyamide material and the cement system.

Firstly, the addition of aluminum sulfate enhances the early strength development of cement by accelerating hydration reactions, promoting crystal nucleation, and improving particle dispersion. These effects make it especially suitable for applications that require rapid strength gain. Secondly, aluminum sulfate also increases the viscosity of cement mixtures and reduces water bleeding, which is advantageous in applications requiring lower fluidity (*e. g.*, casting vertical structures), helping to maintain the desired shape and structural stability.[33]

The accelerator causes an immediate decrease in pH of the pore solution due to the consumption of OH^- ions from the alkaline environment and the subsequent formation of ettringite. This, along with the rapid consumption of Ca^{2+} ions from the pore solution, enhances the dissolution of tricalcium silicate (C_3S) and tricalcium aluminate (C_3A). The increased concentrations of Ca^{2+}, Si^{4+}, and Al^{3+} in the pore solution lead to supersaturation with respect to (calcium aluminat silicate hydrate) C-(A)-S-H, resulting in the nucleation and precipitation of these phases.[34] The accelerator containing aluminum sulfate promotes ettringite formation by accelerating the hydration of C_3S and C_3A during the early stages of cement hydration.[35]

The accelerating effect of $CaCl_2$ is associated with a reduction in hydroxyl ion concentration in the solution.[36] This decrease lowers the system's pH, further facilitating the hydration reactions of C_3S and C_3A. As a result, the formation of calcium silicate hydrate (C-S-H) and ettringite (AFt) is accelerated by the addition of calcium chloride.[37] Juenger *et al.* suggested that $CaCl_2$ promotes the formation of the "inner product" of C-S-H with a low-density microstructure.[38]

Portland cement is often modified with soluble nitrate or nitrite salts to protect reinforcing steel or to shorten setting time. These nitrate and nitrite ions can enter and occupy the anionic sites of AFm, thereby influencing the overall phase balance among cement hydrates. Water that is not incorporated into hydrates remains in the pores and is referred to as "pore water". When soluble anions such as nitrate or nitrite are added to cement, they do not necessarily remain dissolved in the pore fluid. The ability of cement hydrates, such as AFm, to absorb ions also allows solids to incorporate anions, thus affecting their stability in cementitious systems.[39]

Calcium nitrate has been identified as an effective accelerator of cement hydration, leading to faster setting and hardening of concrete.[40] Balonis *et al.* suggested[41] that calcium nitrate can significantly influence the formation and stability of ettringite (AFt) and monosulfate (AFm) phases. The presence of NO_3^- ions in the solution caused phase transitions and the displacement of sulfate ions from monosulfoaluminate (SO_4-AFm), resulting in the formation of NO_3-AFm phases. This transformation contributed to increased cement strength and accelerated hydration.

In this context, the desorption of $Ca^{2+}Cl_2^-$, $Ca^{2+}(NO_3)_2^-$, and $Al^{3+}{}_2(SO_4)^{-2}{}_3$ ions from the surface layers of the polyamide filler into the cement matrix occurs under elevated temperatures generated by the cement hydration process (the exothermic peak temperature of hydration for this cement is approximately 95 ± 5 °C).

Based on these findings, it was decided to limit the modification of polyamide fibers to 30 % solutions of $CaCl_2$ and $Al_2(SO_4)_3$ for further experiments, as these salts showed greater potential to enhance the properties of the cement system.

To study the combined effect of polyamide granules and fibers on the physical and mechanical properties of HSC, polyamide fiber was added to the base concrete mixture at a rate of 1 % by mass relative to the mass of cement (Figs. 10, 11). Fiber-reinforced concrete is increasingly used in the construction industry due to its ability to control cracking and improve both ductility and durability.[42] Randomly oriented fibers form a three-dimensional fibrous network that prevents crack initiation and propagation, primarily due to the adhesion between the fibers and the cement matrix.[43] Improvements in mechanical properties depend on the effectiveness of crack-bridging by the fibers, which is influenced by their geometry, quantity, distribution, modulus of elasticity, and the quality of the fiber–matrix bond.[44] Incorporating fibers with high crack resistance and strength enhances the overall durability and strength of concrete.[45]

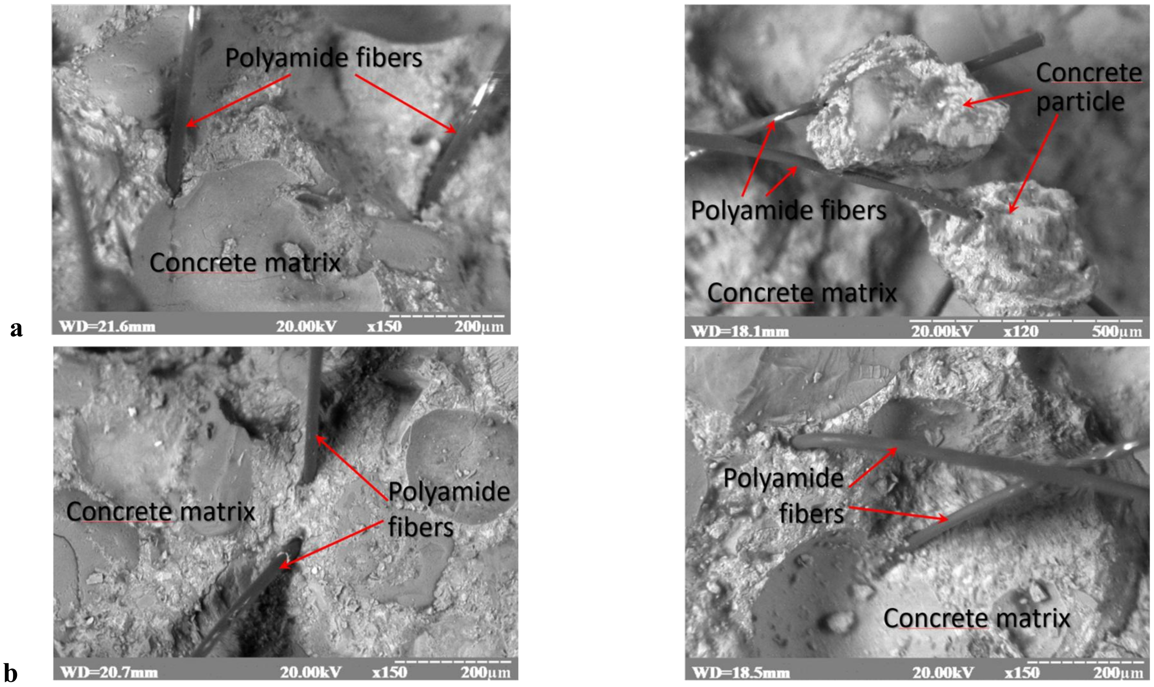

Fig. 10. SEM images of polyamide fibers within the concrete structure:
a – fibers modified in the 30 % $CaCl_2$ solution; b – fibers modified in the 30 % $Al_2(SO_4)_3$ solution

Polyamide (PA) fibers are expected to improve the compressive, tensile, and flexural strength of concrete, as well as its plasticity.[46–48] PA fibers are considered a key component in improving the engineering performance of concrete,[49] contributing to the transition from brittle failure to a more plastic mode of fracture.[50]

Polymer fibers – especially polypropylene fibers – are widely used in concrete technology. Studies by Marushchak *et al.*[51, 52] have shown that adding 1 % by mass of polypropylene fibers can increase the impact strength of concrete up to 200 N. Moreover, engineered cementitious composites reinforced with polypropylene fibers exhibit 29–37 % higher bending strength compared to unreinforced composites. The effect of polypropylene fibers on the tensile behavior of concrete differs significantly from their effect on flexural strength.[53] However, these polymer fibers often have a low modulus of elasticity and limited thermal resistance. Being hydrophobic, polypropylene fibers have limited interaction with the cement matrix.[54, 55] Their low surface free energy and smooth texture result in poor adhesion to concrete, weakening the interfacial bond with the cementitious matrix.[56]

Despite the extensive research on polypropylene fibers, limited attention has been given to the influence of polyamide fibers on the physical and mechanical properties of HSC. To address this gap, a series of experiments was conducted to investigate the effect of polyamide fibers on HSC performance.

The surface properties of polyamide fibers can be enhanced through modification techniques. One effective approach involves increasing the number of functional amino groups via grafting, surface functionalization, or cleavage of amide bonds to form new functional groups.[57]

In this study, polyamide fibers were modified in 30 % solutions of $CaCl_2$ and $Al_2(SO_4)_3$ for 120 hours. Both modified polyamide granules and fibers were incorporated into concrete at rates of 10 % and 1 % by mass of cement, respectively, to improve the physical and mechanical properties of the concrete. As shown in Fig. 10 and Fig. 11, the modified polyamide granules and fibers are evenly distributed within the concrete matrix, contributing to structural reinforcement and strength enhancement.

For the studied concrete composition, which includes granular polyamide modified in a 30 % $CaCl_2$ solution (10.0 % of the cement mass) and polyamide fiber modified in a 30 % $CaCl_2$ solution (1.0 % of the cement mass), the early-age compressive strength was $f_{cs}2$ = 72.8 MPa, increasing to $f_{cs}28$ = 106.4 MPa after 28 days of curing (Fig. 12). The flexural tensile strength of this concrete was $f_{fs}2$ = 8.5 MPa at an early age, increasing to $f_{fs}28$ = 12.5 MPa after 28 days (Fig. 13).

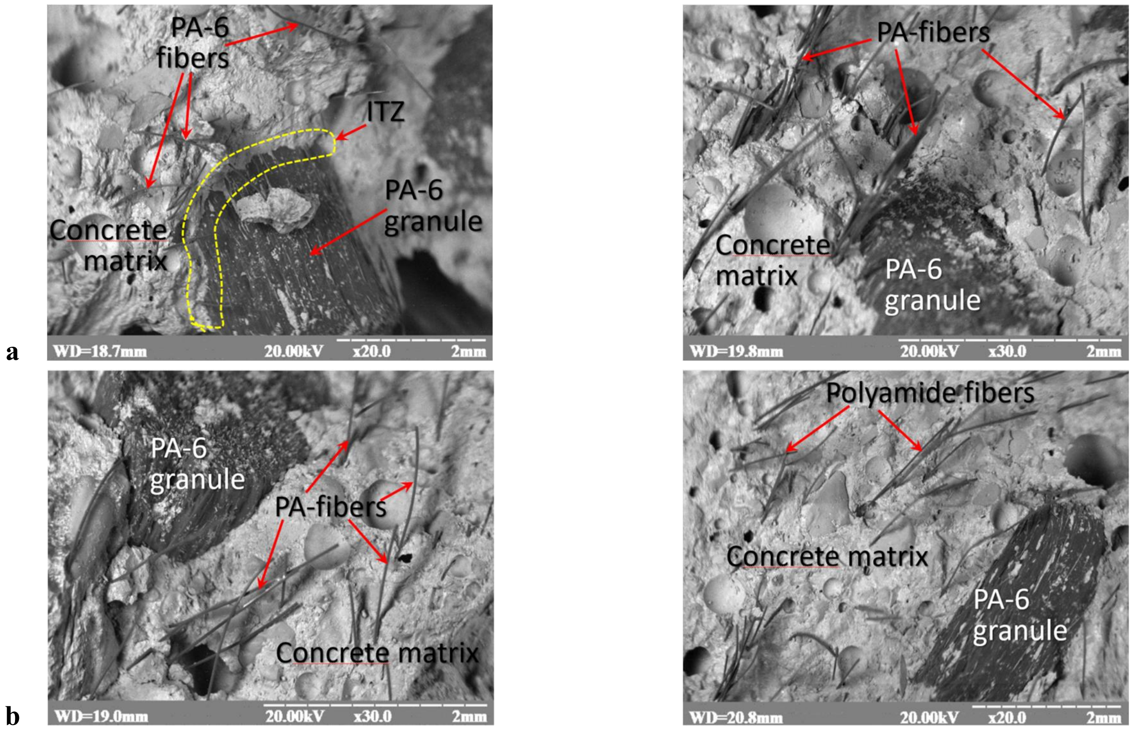

Fig. 11. SEM images of polyamide fibers and PA-6 granules within the concrete structure:
a – polyamide granules and fibers modified in the 30 % $CaCl_2$ solution;
b – polyamide granules and fibers modified in the 30 % $Al_2(SO_4)_3$ solution

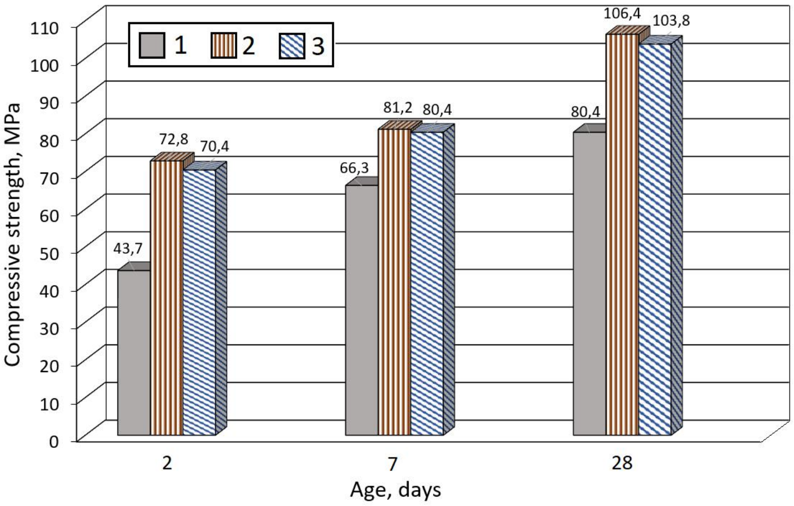

Fig. 12. Compressive strength of concrete samples with the addition of polyamide fibers and polyamide granules: 1 – with the addition of unmodified polyamide granules and fibers, 2 – with the addition of polyamide granules and fibers modified in $CaCl_2$ solution, 3 – with the addition of polyamide granules and fibers modified in $Al_2(SO_4)_3$ solution

For the concrete composition containing granular polyamide modified in a 30 % $Al_2(SO_4)_3$ solution (10.0 % of the cement mass) and polyamide fiber modified in the same solution (1.0 % of the cement mass), the early-age compressive strength was $f_{cs}2$ =70.4 MPa, increasing to $f_{cs}28$ = 103.8 MPa after 28 days of curing (Fig. 12). The flexural tensile strength of this concrete was $f_{fs}2$ = 7.9 MPa at an early age, increasing to $f_{fs}28$ = 10.8 MPa after 28 days (Fig. 13).

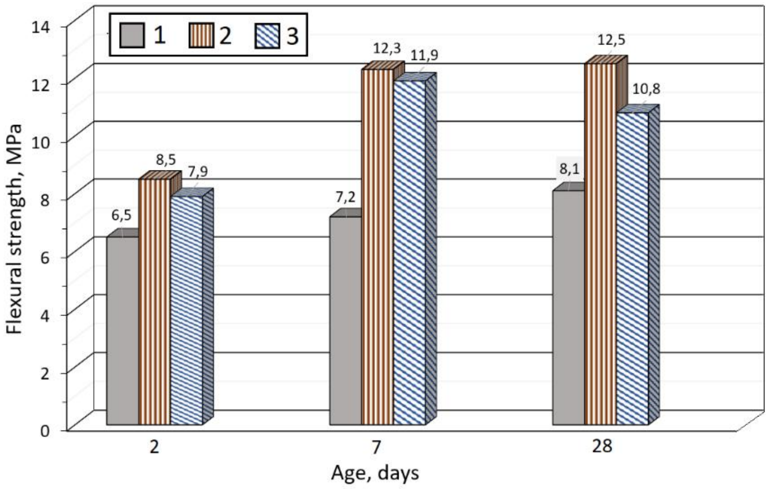

Fig. 13. Flexural tensile strength of concrete samples with the addition of polyamide fibers and polyamide granules: 1 –with the addition of unmodified polyamide granules and fibers, 2 – with the addition of polyamide granules and fibers modified in $CaCl_2$ solution, 3 – with the addition of polyamide granules and fibers modified in $Al_2(SO_4)_3$ solution

To study the effect of polyamide waste on the physical and mechanical properties of high-strength concrete, 10 wt. % of polyamide waste (based on cement mass) was added to the base concrete mix (control composition). Additionally, the polyamide waste was modified in 30 % $CaCl_2$ and 30 % $Al_2(SO_4)_3$ solutions. Both unmodified and salt solution-modified polyamide waste were incorporated into the control mix at 10.0 % of the cement mass. As shown in Fig. 14, the polyamide waste particles are uniformly distributed throughout the concrete matrix and form a continuous contact zone at the "polyamide filler – concrete matrix" interface due to the specific characteristics of their surface. The combined effects of surface roughness, the plate-like shape of the waste particles, and modification in salt solutions contribute to strong bonding between the polyamide waste particles and the cement matrix, resulting in a homogeneous and durable composite material.

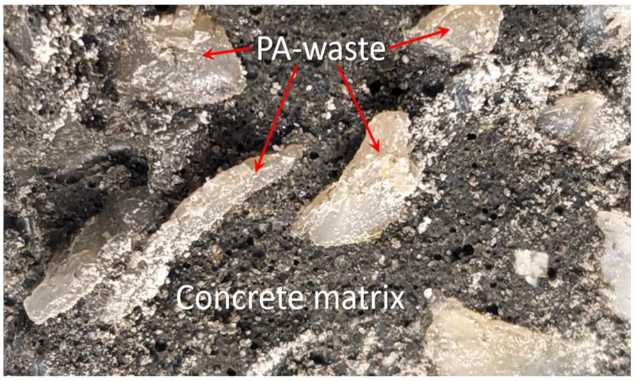

Fig. 14. SEM image of polyamide waste within the concrete structure

For concrete of control composition containing unmodified polyamide waste at 10.0 % of the cement mass, the early-age (2-day) compressive strength was $f_{cs}2$ = 62.4 MPa, increasing to $f_{cs}28$ = 94.3 MPa after 28 days of curing (Fig. 15, *a*). The flexural tensile strength of this concrete was $f_{fs}2$ = 8.7 MPa at an early age and increased to $f_{fs}28$ = 12.2 MPa after 28 days (Fig. 15, *b*). Surface modification of the polyamide waste in 30% $CaCl_2$ solution and 30 % $Al_2(SO_4)_3$ solution improves adhesion with the concrete matrix. This effect is confirmed by the physical and mechanical performance of the concretes containing modified polyamide waste at 10.0 % of the cement mass (Fig. 15, *a*, *b*). For the concrete containing polyamide waste modified in a 30 % $CaCl_2$ solution (10.0 % of the cement mass), the early-age compressive strength was $f_{cs}2$ = 64.4 MPa, increasing to $f_{cs}28$ = 98.4 MPa after 28 days of curing (Fig. 15, *a*). The flexural tensile strength of this concrete was $f_{fs}2$ = 9.2 MPa at an early age and increased to $f_{fs}28$ = 12.9 MPa after 28 days (Fig. 15, *b*). For the concrete containing polyamide waste modified in a 30 % $Al_2(SO_4)_3$ solution (10.0 % of the cement mass), the early-age compressive strength was $f_{cs}2$ = 62.8 MPa, increasing to $f_{cs}28$ = 96.2 MPa after 28 days of curing (Fig. 15, *a*). The flexural tensile strength of this concrete was $f_{fs}2$ = 8.8 MPa at an early age and increased to $f_{fs}28$ = 12.5 MPa after 28 days (Fig. 15, b).

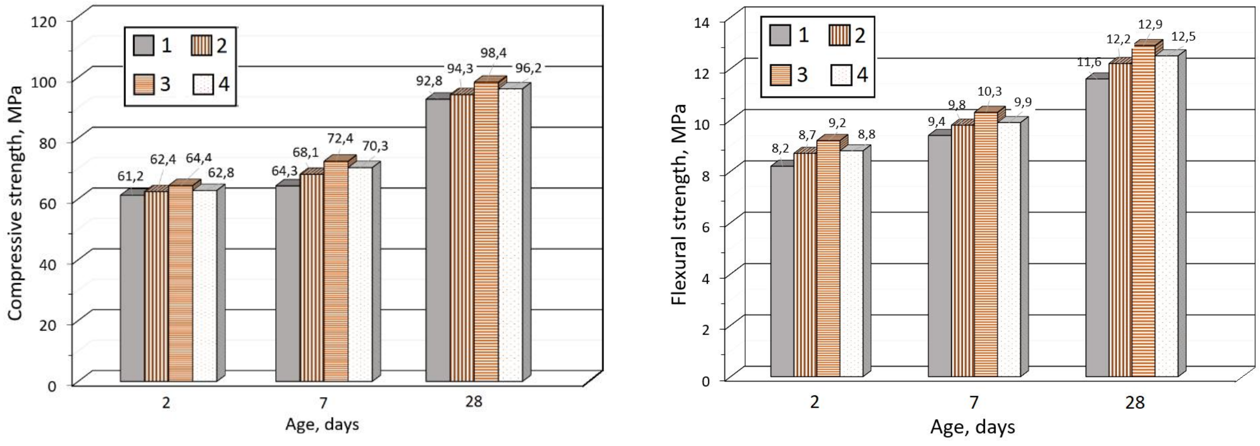

a b

Fig. 15. Compressive strength (a) and flexural tensile strength (b) of concrete samples with the addition of polyamide waste: 1 – without polyamide waste; 2 – with the addition of unmodified polyamide waste; 3 – with the addition of polyamide waste modified in $CaCl_2$ solution, 4 – with the addition of polyamide waste modified in $Al_2(SO_4)_3$ solution

High-strength concretes have been developed based on cementitious systems modified with granulated polyamide and polyamide fibers. These concretes exhibit enhanced structural and technical properties, making them suitable for potential applications in the construction of structural layers of road pavements,[58] as well as in the production of high-performance cement composites with improved physical and mechanical characteristics.[59–61] It has been demonstrated that similar interaction patterns between the surface of the polyamide filler and the concrete matrix, along with improvements in concrete performance, are also observed when using polyamide waste as a filler – especially when it is modified with inorganic salt solutions. Moreover, the use of polyamide waste in concrete not only increases its mechanical strength but also contributes to solving environmental problems associated with polymer waste disposal.

4. Conclusions

This study investigated the influence of various types of polyamide fillers (granules, fibers, and plate-like waste) on the physical and mechanical properties of high-strength concrete. It was found that incorporating polyamide fillers into the concrete structure consistently leads to increases in both strength and plasticity. Furthermore, it was demonstrated that additional modification of polyamide fillers with $CaCl_2$, $Al_2(SO_4)_3$, and $Ca(NO_3)_2$ solutions enhances the overall performance of the concrete.

When PA-6 granules were used as a filler, the highest early compressive strength recorded was $f_{cs}2$ = 61.5 MPa, increasing to $f_{cs}28$ = 103.6 MPa after 28 days of curing. This result was observed in concrete containing 10 wt. % of PA-6 granules modified in a $CaCl_2$ solution. In contrast, the lowest compressive strength was observed in concrete with 10 wt. % of PA-6 granules modified in distilled water – $f_{cs}2$ = 40.7 MPa at an early age and $f_{cs}28$ = 72.8 MPa after 28 days.

It was established that the most significant improvement in the physical and mechanical properties of concrete was achieved using a combined filler – the mixture of polyamide granules and fibers modified with inorganic salts. In this case, the highest early compressive strength reached $f_{cs}2$ = 72.8 MPa, increasing to $f_{cs}28$ = 106.4 MPa after 28 days. This performance was achieved in concrete containing 10 wt. % of PA-6 granules and 1.0 wt. % of polyamide fibers (by cement mass), both modified in a 30 % $CaCl_2$ solution.

It has also been shown that similar interaction patterns between the polyamide filler surface and the concrete matrix, as well as comparable improvements in concrete performance, occur when polyamide waste is used – particularly after modification in inorganic salt solutions. In addition to improving mechanical strength, the use of polyamide waste in concrete offers an environmentally sustainable approach to polymer waste recycling.

The obtained results indicate that incorporating modified polyamide fillers into concrete is an effective method for creating composite materials (concretes) with enhanced physical-mechanical properties. Considering the interaction of the filler surface with concrete, the significantly lower density and weight of polyamide compared to steel, and the susceptibility of steel reinforcement to corrosion in reinforced concrete, the results obtained are promising for the development of polyamide reinforcement, particularly from polymer waste.

The results confirm that incorporating modified polyamide fillers into concrete is an effective strategy for developing composite materials with enhanced physical and mechanical properties. Considering the beneficial interaction of the filler surface with the concrete matrix, the significantly lower density and weight of polyamide compared to steel, and the vulnerability of steel reinforcement to corrosion, these findings highlight the potential of polyamide-based reinforcement – especially from recycled polymer waste – as a promising direction for future development.

References

[1] Bušić, R; Miličević, I; Rakocija, I; Mendeš, A. Experimental Investigation on Workability and Mechanical Properties of Carbon Fiber Reinforced High-Strength Concrete (HSC) Containing Waste Bakelite Aggregate (WBA). *Mater Today: Proc.* **2023**, *6*, 131. https://doi.org/10.1016/j.matpr.2023.06.151

[2] Hashim, Y.; Yang, Q.; Li, P. Load Path Dependence for Passively and Actively Confined High-Strength Concrete.*Constr Build Mater*. **2024**, *440*, 137353. https://doi.org/10.1016/j.conbuildmat.2024.137353

[3] Sidhu, A.; Siddique, R. Review on Effect of Curing Methods on High Strength Concrete. *Constr Build Mater*. **2024**, *438*, 136858. https://doi.org/10.1016/j.conbuildmat.2024.136858

[4] Guan, Z.; Lai, Z.; Qin, J.; Chen, Y.; Wen, Y.; Huang, R. Mechanical Properties of High-Strength Concrete (HSC) under Projectile Penetration. *Constr Build Mater*. **2024**, *442*, 137579. https://doi.org/10.1016/j.conbuildmat.2024.137579

[5] Ahmad, M.; Rizwan, M.; Javed, M.; Alkhattabi, L.; Aslam, F.; Qamar, M.; Ullah, F. Optimizing Hybrid Fiber Content for Enhanced Thermo-Mechanical Performance of High-Strength Concrete. *Mater Today Commun*. **2024**, *39*, 109293. https://doi.org/10.1016/j.mtcomm.2024.109293

[6] Du, T.; Liu, F.; Wei, H.; Li, Y.; Yang, H.; Peng, K. Behaviours of Circular High-Strength Concrete-Filled High-Strength Steel Tubular Columns after Constant Heating. *J Constr Steel Res*. **2024**, *221*, 108933. https://doi.org/10.1016/j.jcsr.2024.108933

[7] Shevchenko, V.; Kotsay, G. Influence of Fine-Grinded Glass Additives on the Induction and Post-induction Periods of Portland Cement Hardening. *Chem. Chem. Technol.* **2014**, *8*, 189–192. https://doi.org/10.23939/chcht08.02.189

[8] Pakravan, H.R; Ozbakkaloglu, T. Synthetic Fibers for Cementitious Composites: A Critical and in-Depth Review of Recent Advances. *Constr Build Mater.* **2019**, *207*, 491–518. https://doi.org/10.1016/j.conbuildmat.2019.02.078

[9] Kabat, O.; Boiko, Yu. Polymer Composites Based on Aromatic Polyamide and Aramid Fiber for Heavy-Duty Friction and Sealing Units. *Chem. Chem. Technol.* **2025**, *19*, 335–341. https://doi.org/10.23939/chcht19.02.335

[10] Suberlyak, O.; Grytsenko, O.; Baran, N.; Yatsulchak, G.; Berezhnyy, B. Formation Features of Tubular Products on the Basis of Composite Hydrogels. *Chem. Chem. Technol.* **2020**, *14*, 312–317. https://doi.org/10.23939/chcht14.03.312

[11] Suberlyak, O. V.; Baran, N. M.; Melnyk, Y. Y.; Grytsenko, O. M.; Yatsulchak, H. V. Influence of the Molecular Weight of Polyvinylpyrrolidone on the Physicomechanical Properties of Composite Polyamide Hydrogel Membranes. *Mater Sci*. **2020**, *55*, 758–764. https://link.springer.com/article/10.1007/s11003-020-00368-3

[12] Baran, N.; Grytsenko, O.; Dulebova, L.; Spišak, E. Features of the Formation of a Reinforcing Coating on Hydrogel Membranes Based on Polyvinylpyrrolidone Copolymers. *Appl Sci.* **2024**, *14*, 3234. https://doi.org/10.3390/app14083234

[13] Kabat, O.; Sytar, V.; Sukhyy, K. Antifrictional Polymer Composites Based on Aromatic Polyamide and Carbon Black. *Chem. Chem. Technol.* **2018**, *12*, 326–330. https://doi.org/10.23939/chcht12.03.326

[14] Caballero, B. M.; Lopez-Urionabarrenechea, A.; Gonzalez-Arcos, J. P.; Perez-Martinez, B. B.; Acha, E.; Iturrondobeitia, M.; Ibarretxe, J.; Esnaola, A.; Baskaran, M. Recycling Fiber-Reinforced Polyamide Waste from the Automotive Industry: Life Cycle Assessment (LCA) of an Advanced Pyrolysis Process to Reclaim Glass Fibers and Valuable Chemicals. *Materials.* **2025**, *18*, 1594. https://doi.org/10.3390/ma18071594

[15] Kim, K.; Kim, M.; Kim, Y.; Kim, J.; Lim, J.; Lee, W.; Kim, H.S.; Cho, D.-H.; Lee, J.; Choi, S. Melt Spinnability Comparison of Mechanically and Chemically Recycled Polyamide 6 for Plastic Waste Reuse. *Polymers.* **2024**, *16*, 3152. https://doi.org/10.3390/polym16223152

[16] Gama, N.; Araújo, J.; Godinho, B.; Ferreira, A.; Barros-Timmons, A. Solvolysis of Nylon: A Pathway to Sustainable Recycling and Circular Economy. *Sustainability.* **2024**, *16*, 9725. https://doi.org/10.3390/su16229725

[17] Kazemi, M.; Kabir, Sk. F.; Fini, E. Review State of the Art in Recycling Waste Thermoplastics and Thermosets and their Applications in Construction. *Resour Conserv Recycl.* **2021**, *174*, 105776. https://doi.org/10.1016/j.resconrec.2021.105776

[18] Colangelo, F.; Cioffi, R.; Liguori, B.; Iucolano, F. Recycled Polyolefins Waste as Aggregates for Lightweight Concrete. *Composites, Part B.* **2016**, *106*, 234–241. https://doi.org/10.1016/j.compositesb.2016.09.041

[19] Lee, J.; Kim, J.; Ahn, J.; Ahn, Y.; Lee, S. Current Advancements in the Bio-Based Production of Polyamides. *Trends Chem.* **2023**, *12*, 873–891. https://doi.org/10.1016/j.trechm.2023.10.001

[20] Kabat, O.; Sytar, V.; Derkach, O.; Sukhyy, K. Polymeric Composite Materials of Tribotechnical Purpose with a High Level of Physical, Mechanical and Thermal Properties. *Chem. Chem. Technol.* **2021**, *15*, 543–550. https://doi.org/10.23939/chcht15.04.543

[21] Zhang, Q.; Zhu, G.-R.; Xiao, X.-X.; Jiang, M.; He, F.-M.; Li, X.; Guo, D.; Zhao, H.B.; Zhao, Z.-Y.; Chen, L.; *et al.* Room-Temperature Hydrogen Bonding and High-Temperature Rearrangement towards High-Performance Flame-Retardant Aliphatic Polyamide. *Polymer.* **2024**, *295*, 126780. https://doi.org/10.1016/j.polymer.2024.126780

[22] Kijo-Kleczkowska, A.; Szumera, M.; Gnatowski, A.; Sadkowski, D. Comparative Thermal Analysis of Coal Fuels, Biomass, Fly Ash and Polyamide. *Energy.* **2022**, *258*, 124840. https://doi.org/10.1016/j.energy.2022.124840

[23] Dencheva, N.; Nunes, T.; Oliveira, M.; Denchev, Z. Microfibrillar Composites Based on Polyamide/Polyethylene Blends. 1. Structure Investigations in Oriented and Isotropic Polyamide 6. *Polymer.* **2005**, *46*, 887–901. https://doi.org/10.1016/j.polymer.2004.11.105

[24] Abdel-Maksoud, G.; Mohamed, O.; Mohamed, W.; Elnagar, K.; Abdallah, A.; Youssef, R.; Elsayed, D.; Labib, N.; Bayoumy, A.; Elhaes, H.; *et al.* Physical Prospective of Polyamide 6 for the Consolidation of Fragile Vegetable Tanned Leather Artifacts. *J Cult Heritage*. **2024**, *67*, 32–41. https://doi.org/10.1016/j.culher.2024.02.002

[25] Krylova, V.; Dukštienė, N. The Structure of PA-Se-S-Cd Composite Materials Probed with FTIR Spectroscopy. *Appl Surf Sci*. **2019**, *470*, 462–471. https://doi.org/10.1016/j.apsusc.2018.11.121

[26] Dasgupta, S.; Hammond, W. B.; Goddard III, W. A. Crystal Structures and Properties of Nylon Polymers. *J Am Chem Soc*. **1996**, *118*, 12291–12301.

[27] Zope, I. S.; Dasari, A.; Guan, F.; Yu, Z-Z. Influence of Metal Ions on Thermo-Oxidative Stability and Combustion Response of Polyamide 6/Clay Nanocomposites. *Polymer.* **2016**, *92*, 102–113. https://doi.org/10.1016/j.polymer.2016.03.087

[28] Al-Mansour, A.; Zhu, Y.; Lan, Y.; Dang, N.; Alwathaf, A.; Zeng, Q. Improving the Adhesion between Recycled Plastic Aggregates and the Cement Matrix. In *Reuse of Plastic Waste in Eco-Efficient Concrete*; Edited by: Pacheco-Torgal, F.; Khatib, J., Eds.; Elsevier, 2024; pp. 113–138. https://doi.org/10.1016/B978-0-443-13798-3.00008-5

[29] Ksouri, I.; de Almeida, O.; Haddar, N. Long Term Ageing of Polyamide 6 and Polyamide 6 Reinforced with 30 % of Glass Fibers: Physicochemical, Mechanical and Morphological Characterization. *J Polym Res*. **2017**, *24*, 133. https://doi.org/10.1007/s10965-017-1292-6.

[30] Hou, Y. The Moisture Absorption of 3D Printed Short Carbon Fibre Reinforced Polyamide. *Composites, Part A*. **2024**, *184*, 108266. https://doi.org/10.1016/j.compositesa.2024.108266

[31] Venoor, V.; Park, J. H.; Kazmer, D. O.; Sobkowicz, M. J. Understanding the Effect of Water in Polyamides: A Review. *Polym Rev*. **2020**, *61*, 598–645. https://doi.org/10.1080/15583724.2020.1855196

[32] Thirumalai, R.; Løgstrup, D. P.; Andersen, T., & Lystrup, A. Influence of Moisture Absorption on Properties of Fiber Reinforced Polyamide 6 Composites. In *Proceedings of the 26th Annual Technical Conference of the American Society for Composites 2011 and the 2nd Joint US-Canada Conference on Composites*; **2011**, 1; pp 500–510.

[33] Meng, Li-Yi; Wang, Y.-S.; Lin, R.; Wang, X.-Y. The Influence and Mechanism Analysis of Aluminum Sulfate as an Environmentally Friendly Early Strength Agent on the Properties of Cement-Based Materials. *Case Stud Constr Mater*. **2024**, *20*, e03278. https://doi.org/10.1016/j.cscm.2024.e03278

[34] Briendl, L. G.; Mittermayr, F.; Baldermann, Andre; Steindl, F. R.; Sakoparnig, M.; Letofsky-Papst, I.; Galan, I. Early Hydration of Cementitious Systems Accelerated by Aluminium Sulphate: Effect of Fine Limestone. *Cem Concr Res*. **2020**, *134*, 106069. https://doi.org/10.1016/j.cemconres.2020.106069

[35] Liu, X.; Ma, B.; Tan, H.; Gu, B.; Zhang, T.; Chen, P.; Li, H.; Mei, J. Effect of Aluminum Sulfate on the Hydration of Portland Cement, Tricalcium Silicate and Tricalcium Aluminate. *Constr Build Mater*. **2020**, *232*, 117179. https://doi.org/10.1016/j.conbuildmat.2019.117179

[36] Kishar, E. A; Ahmed, D. A; Mohammed, M. R; Noury, R. Effect of Calcium Chloride on the Hydration Characteristics of Ground Clay Bricks Cement Pastes. *Beni-Suef Univ. J. Basic Appl. Sci.* **2013**, *2*, 20–30. https://doi.org/10.1016/j.bjbas.2013.09.003

[37] Zhao, B.; Wen, J.; Zhai, D.; Tang, R; Chen, S.; Xin, J. Effect of Calcium Chloride on the Properties of Gangue Cemented Paste Backfill: Experimental Results of Setting Time, Rheological Properties, Mechanical Strength and Microscopic Properties. *Case Stud Constr Mater*. **2025**, *22*, e04331. https://doi.org/10.1016/j.cscm.2025.e04331

[38] Juenger, M. C. G.; Monteiro, P. J. M.; Gartner, E. M.; Denbeaux, G. P. A Soft X-ray Microscope Investigation into the Effects of Calcium Chloride on Tricalcium Silicate Hydration. *Cem Concr Res*. **2005**, *35*, 19–25.

[39] Balonis, M. Solid Solutions Among Cement AFm Phases Containing Nitrate and Nitrite Ions. *Adv Cem Res*. **2023**, *36*, 337–358. https://doi.org/10.1680/jadcr.23.00010

[40] Zhuo, C.; Yishun, L; Fang, D.; Kejin, W.; Tianxiao, Z.; Haibao, W. Effect of Calcium Nitrate on Hydration Properties and Strength Development of Calcium Sulfoaluminate Cement. *Constr Build Mater*. **2024**, *421*, 135770. https://doi.org/10.1016/j.conbuildmat.2024.135770

[41] Balonis, M.; Mędala, M.; Glasser, F. P. Influence of Calcium Nitrate and Nitrite on the Constitution of AFm and AFt Cement Hydrates. *Adv Cem Res*. **2011**, *23*, 129–143. https://doi.org/10.1680/adcr.10.00002

[42] Saatci, S.; Sirin Cetin, F.; Sarra Aloui, S.; Naseri, J. Effects of Steel Fiber Type and Ratio on the One-Way Bending Behavior of Hybrid Fiber Reinforced Concrete Thin Panels. *Constr Build Mater*. **2024**, *411*, 134190. https://doi.org/10.1016/j.conbuildmat.2023.134190

[43] Wang, S.; Wang, B.; Zhu, H.; Chen, G.; Li, Z.; Yang, L.; Zhang, Y.; Zhou, X. Ultra-High Performance Concrete: Mix Design, Raw Materials and Curing Regimes-A Review. *Mater Today Commun*. **2023**, *35*, 105468. https://doi.org/10.1016/j.mtcomm.2023.105468

[44] Fu, B.; Xu, G.-T.; Peng, W.-S.; Huang, J.-Z.; Zou, Q.-Q.; Kuang, Y.-D. Performance Enhancement of Recycled Coarse Aggregate Concrete by Incorporating with Macro Fibers Processed from Waste GFRP. *Constr Build Mater*. **2024**, *411*, 134166. https://doi.org/10.1016/j.conbuildmat.2023.134166

[45] Liang, N.; Geng, S.; Mao, J.; Liu, X.; Zhou, X. Investigation on Cracking Resistance Mechanism of Basalt-Polypropylene Fiber Reinforced Concrete Based on SEM Test. *Constr Build Mater*. **2024**, *411*, 134102. https://doi.org/10.1016/j.conbuildmat.2023.134102

[46] Du, J.; Meng, W.; Khayat, K. H.; Bao, Y.; Guo, P.; Lyu, Z.; Abu-obeidah, A.; Nassif, H.; Wang, H. New Development of Ultra-High-Performance Concrete (UHPC). *Composites, Part B*. **2021**, *224*, 109220, https://doi.org/10.1016/j.compositesb.2021.109220

[47] Cavusoglu, I.; Yilmaz, E.; Yilmaz, A. Additivity Effect on Properties of Cemented Coal Fly Ash Backfill Containing Water-Reducing Admixtures. *Constr Build Mater*. **2021**, *267*, 121021, https://doi.org/10.1016/j.conbuildmat.2020.121021

[48] Wang, S.; Zhu, H.; Liu, F.; Cheng, S.; Wang, B.; Yang, L. Effects of Steel Fibers and Concrete Strength on Flexural Toughness of Ultra-High Performance Concrete with Coarse Aggregate. *Case Stud Constr Mater*. **2022**, *17*, e1170, https://doi.org/10.1016/j.cscm.2022.e01170

[49] Jang, E.; Kim, J. J.; Yoo, D. Dynamic Pullout Behavior of Multiple Steel Fibers in UHPC: Effects of Fiber Geometry, Inclination Angle, and Loading Rate. *Materials*. **2019**, *12*, 3365. https://doi.org/10.3390/ma12203365

[50] Ren, L.; Fang, Z.; Wang, K. Design and Behavior of Super-Long Span Cable-Stayed Bridge with CFRP Cables and UHPC Members. *Composites, Part B*. **2019**, *164*, 72–81. https://doi.org/10.1016/j.compositesb.2018.11.060

[51] Marushchak, U.; Sydor, N.; Margal, I. Impact of Polypropylene Fibers on the Properties of Engineered Cementitious Composites. *Lecture Notes in Civ Eng*. **2023**, *290*, 262–269. https://doi.org/10.1007/978-3-031-14141-6_26

[52] Marushchak, U.; Sydor, N.; Braichenko, S.; Margal, I.; Soltysik, R. Modified Fiber Re-Inforced Concrete for Industrial Floors. *IOP Conference Series: Mater Sci Eng*. **2019**, *708*, 012094. https://doi.org/10.1088/1757-899X/708/1/012094

[53] Hassan, A.; El Nemr, A.; Goebel, L.; Koenke, C. Effect of Hybrid Polypropylene Fibers on Mechanical and Shrinkage Behavior of Alkali-Activated Slag Concrete. *Constr. Build Mater*. **2024**, *411*, 134485. https://doi.org/10.1016/j.conbuildmat.2023.134485

[54] Richardson, A. Compressive Strength of Concrete with Polypropylene Fibre Additions. *Struct Surv*. **2006**, *24*, 138–153. https://doi.org/10.1108/02630800610666673

[55] Tran, T.; Pham, T.; Huang, Z.; Chen, W.; Hao, H.; Elchalakani, M. Impact Response of Fibre Reinforced Geopolymer Concrete Beams with BFRP Bars and Stirrups. *Eng. Struct*. **2021**, *231*, 111785. https://doi.org/10.1016/j.engstruct.2020.111785

[56] Hao, Y.; Cheng, L.; Hao, H.; Shahin, M. Enhancing Fiber/Matrix Bonding in Polypropylene Fiber Reinforced Cementitious Composites by Microbially Induced Calcite Precipitation pre-Treatment. *Cem Concr Compos*. **2018**, *88*, 1–7. https://doi.org/10.1016/j.cemconcomp.2018.01.001

[57] Stiegelmaier, E.; Costa, T. C.; Pakuszewski, G.; Guelli Ulson de Souza, S. M.; Ulson de Souza, A. A.; Serafini Immich, A. P. Enhancing Polyamide 6: Acid Hydrolysis for Functionalization and Amino Group Quantification. *Polymer*. **2024**, *298*, 126905. https://doi.org/10.1016/j.polymer.2024.126905

[58] Novytskyi, Y.; Topylko, N.; Marushchak, U.; Turba, Y. Composite Materials Based on Phosphogypsum for Constructive Layers of Road Pavement. *Chem. Chem. Technol.* **2024**, *18*, 7–15. https://doi.org/10.23939/chcht18.01.007

[59] Kropyvnytska, T.; Sanytsky, M.; Kaminskyi, A.; Vakhula, O. Effect of Layered Double Hydroxides Ca-Al LDHs and Polycarboxylate Ethers on the Hardening of Portland Limestone Cement. *Eastern-European J. Enterp. Technol.* **2022**, *5*(6(119), 30–40. https://doi.org/10.15587/1729-4061.2022.266269

[60] Sanytsky, M.; Kropyvnytska, T.; Vakhula, O.; Bobetskyi, Y. Nanomodified Ultra High-Performance Fiber Reinforced Cementitious Composites with Enhanced Operational Characteristics. In *Proceedings of CEE 2023. CEE 2023. Lecture Notes in Civil Engineering, vol 438*; Blikharskyy, Z.; Koszelnik, P.; Lichołai, L.; Nazarko, P.; Katunský, D., Eds.; Springer, Cham., 2023. https://doi.org/10.1007/978-3-031-44955-0_36

[61] Vakhula, O.; Kindzera, D.; Novytskyi, Y. Study of the Influence of Polycarboxylate Type Superplasticizers MasterGlenium ACE 430 and MasterGlenium ACE 560 on the Physical and Technical Properties of Fine-Grained Concrete. *Chem. Chem. Technol.* **2025**, *19*, 286–296. https://doi.org/10.23939/chcht19.02.286

Received: May 08, 2025 / Revised: July 08, 2025 / Accepted: September 02, 2025

ДОСЛІДЖЕННЯ ВПЛИВУ ПОЛІАМІДНОГО НАПОВНЮВАЧА НА ФІЗИКО-МЕХАНІЧНІ ВЛАСТИВОСТІ ВИСОКОМІЦНИХ БЕТОНІВ

Анотація. *У статті досліджено вплив різних поліамідних наповнювачів (гранульований поліамід PA-6, поліамідні волокна та поліамідні відходи) на фізико-механічні властивості високоміцного бетону. Встановлено, що модифікація поверхні наповнювачів у розчинах неорганічних солей ($CaCl_2$, $Al_2(SO_4)_3$, $Ca(NO_3)_2$) дає змогу впливати на гідратаційні процеси цементної матриці та покращує міжфазну взаємодію, що, своєю чергою, підвищує міцність і довговічність бетонів. Найвищої міцності на стиск ($f_{cs}2 = 72,8$ МПа; $f_{cs}28 = 106,4$ МПа) досягнуто із використанням 10 мас. % гранул поліаміду PA6 та 1,0 мас. % фібри, модифікованих у 30 % розчині $CaCl_2$. Таке поєднання забезпечує ефективне армування структури бетону, знижує ймовірність утворення тріщин і сприяє покращенню експлуатаційних властивостей. Крім того, використання поліамідних відходів як наповнювача є перспективним напрямом утилізації полімерних матеріалів із позитивним екологічним ефектом.*

Ключові слова: *цементна система, високоміцний бетон, поліамід, поліамідне волокно, поліамідні відходи, міцність.*